

Large-scale *de novo* prediction of physical protein-protein association

Antigoni Elefsinioti^{1,6}, Ömer Sinan Saraç¹, Anna Hegele², Conrad Plake¹, Nina C. Hubner^{3,7}, Ina Poser⁴, Mihail Sarov⁴, Anthony Hyman⁴, Matthias Mann³, Michael Schroeder¹, Ulrich Stelzl², Andreas Beyer^{1,5}

Affiliations:

1. Biotechnology Center, TU Dresden, Dresden, Germany
2. Otto-Warburg Laboratory, Max-Planck Institute for Molecular Genetics, Berlin, Germany
3. Dept. of Proteomics and Signal Transduction, Max-Planck Institute for Biochemistry, Martinsried, Germany
4. Max-Planck Institute of Molecular Cell Biology and Genetics, Dresden, Germany
5. Center for Regenerative Therapies Dresden, TU Dresden, Dresden, Germany
6. Current Affiliation: Max Delbrück Center for Molecular Medicine, Berlin-Buch, Germany
7. Current Affiliation: Molecular Cancer Research, University Medical Centre Utrecht, Utrecht, The Netherlands

Corresponding Author:

Andreas Beyer
Biotechnology Center
TU Dresden
Tatzberg 47/49
01307 Dresden
Germany

Phone: +49-351-463 40080
FAX: +49-351-463 40087
E-Mail: andreas.beyer@biotec.tu-dresden.de

Running title: Large-scale prediction of protein interactions

Abbreviations used: ALS, amyotrophic lateral sclerosis; APMS, affinity purification-mass spectrometry; CNS, central nervous system; CORUM, the Comprehensive Resource of Mammalian protein complexes; GAD, Genetic Association Database; GWAS, genome-wide association studies; HPRD, the Human Protein Reference Database; KEGG, Kyoto Encyclopedia of Genes and Genomes; OMIM, Online Mendelian Inheritance in Man; QUBIC, Quantitative BAC InteraCtomics; STRING, Search Tool for the Retrieval of Interacting Genes ;Y2H, yeast two-hybrid

Abstract

Information about the physical association of proteins is extensively used for studying cellular processes and disease mechanisms. However, complete experimental mapping of the human interactome will remain prohibitively difficult in the near future.

Here we present a map of predicted human protein interactions that distinguishes functional association from physical binding. Our network classifies more than 5 million protein pairs predicting 94,009 new interactions with high confidence. We experimentally tested a subset of these predictions using yeast two-hybrid analysis and affinity purification followed by quantitative mass spectrometry. Thus we identified 462 new protein-protein interactions and confirmed the predictive power of the network. These independent experiments address potential issues of circular reasoning and are a distinctive feature of this work. Analysis of the physical interactome unravels subnetworks mediating between different functional and physical sub-units of the cell. Finally, we demonstrate the utility of the network for the analysis of molecular mechanisms of complex diseases by applying it to genome wide association studies of neurodegenerative diseases. This analysis provides new evidence implying TOMM40 as a factor involved in Alzheimer's disease.

The network provides a high-quality resource for the analysis of genomic datasets and genetic association studies in particular. Our interactome is available via the hPRINT web server at: www.print-db.org.

Introduction

Accurate high-throughput detection of protein-protein interactions is one of the most challenging tasks in the post-genomic era. Availability of such data has become essential for studying biological pathways, molecular evolution, for assessing protein functions based on functional genetics screens, and for studying molecular mechanisms of diseases (1-3). The size of the human physical interactome is predicted to be between 130,000-600,000 interactions (2, 4, 5). High throughput techniques, such as yeast two-hybrid (Y2H) (6, 7) or affinity purification followed by mass spectrometry (8, 9) are being used for the large-scale measurement of protein binding. However, those interactions, together with the protein-protein interactions measured through small-scale experiments (10) only cover 52,000 interactions, i.e. less than 25% of the predicted human interactome (11). Computational prediction of protein interactions can fill this gap until the human interactome has been fully explored using experimental techniques (12). In addition, computational prediction can help guiding experimental screening thereby significantly shortening the time needed until reaching (nearly) complete coverage of an interactome (13).

It is important to distinguish databases assembling data and reporting experimentally tested interactions from others that actually predict previously not reported interactions. We call the second type of interactions 'de novo' predictions, as these interactions have no experimental evidence through assays directly testing for binding (although there might be indirect experimental evidence, e.g. co-expression or common knock-out phenotypes). The class of databases making such de novo prediction can again be sub-divided in two subtypes: those predicting functional interactions (14-16) and others predicting physical association (14, 17-20). A functional interaction typically just indicates membership in a common pathway, whereas physical association refers to direct or indirect binding of proteins in a stable or transient complex. Recent work has underlined the importance of distinguishing the prediction of functional from physical association (19-21). Knowing physical associations is important for elucidating the structure of pathways and for understanding molecular

mechanisms underlying high-level phenotypes (1, 4, 11). However, only few existing databases actually make computational predictions of physical associations of human proteins using heterogeneous types of evidence (18-20).

Here we present an approach that integrates heterogeneous biological data in order to predict and distinguish physical from functional interactions. Applying this framework to human data we were able to predict 94,009 new physical associations with high confidence (probability > 0.7, see *Results* for more details). We termed this map 'human predicted protein interactome' (hPRINT) and validated predictions experimentally based on yeast two-hybrid (Y2H) and AP-MS analyses. Using these complementary technologies we identified 462 new human protein interactions and we validated the high predictive power of our scoring scheme.

Having established the accuracy of hPRINT, we used this interaction map for studying the physical organization of cellular processes with a specific focus on the molecular causes of neurodegenerative diseases. Our assessment of interactions between gene products that are associated with neurodegenerative diseases reveals that hPRINT can be used for prioritizing candidate genes suggested by genome-wide association studies. Using amyotrophic lateral sclerosis (ALS), Alzheimer's and Parkinson's diseases as examples we demonstrate how hPRINT can assist in the reconstruction of molecular mechanisms linking genes to pathologic phenotypes.

Experimental Procedures

Interaction Prediction

Datasets

For training and testing, we used data from HPRD (22), CORUM (23), and KEGG (24). In order to create a dataset of physically interacting genes (PHYSET, 72450 interactions), we selected only *in vivo* interactions from HPRD, human interactions from CORUM and binary and complex interactions defined in human KEGG pathways. In addition, we selected high confidence interactions reported in a previous analysis (25) where each interaction is reported in at least two publications (termed CRGhigh). A dataset of functionally related but not physically interacting genes (FUNSET, 412,587 interactions) was extracted from KEGG pathways. FUNSET is composed of gene pairs that are in the same pathway but are not physically interacting. Finally we generated a dataset of non-interacting gene pairs (NONSET, 331,596 interactions). NONSET consists of random pairs of genes from distinct KEGG pathways that are not known to interact physically. Hence, NONSET represents interactions that are neither functionally related nor physically binding.

Feature Set

We used 18 features to predict interactions. Five types of evidence are taken from the STRING database (version 8.2): genomic neighborhood, gene fusion, phylogenetic profile, coexpression, and text mining (16). Five additional features are generated using the GoGene tool which annotates genes based on Gene Ontology (GO) terms and disease annotations using text mining information (including co-occurrence in publications) (26). The features extracted with GoGene are: cellular component, molecular function, biological process, disease, co-occurrence. Next, we used presence of known binding motifs in protein sequences as a predictor for physical binding. This feature (named 'domain pairs') is based on the presence of binding domains predicted by profile Hidden Markov Models (HMM) (27). Finally, we considered the topology of the STRING interaction network to

predict physical interactions. We re-calculated the STRING combined score after eliminating the *experimental* and *database* features in order to exclude any experimental evidence. Using the resulting STRING interaction scores we extracted seven topological features for each edge of this network: clustering coefficient, minimum spanning tree, extended minimum spanning tree, neighborhood ratio, ratio between shortest path and edge weight, local betweenness, and global betweenness. Detailed descriptions for all features can be found in supplementary material.

Training

We performed three-class classification, namely physical, functional and non-related. All the PHYSET is used as training data for physical interactions. To avoid a bias towards larger classes, we randomly sampled from FUNSET and NONSET to obtain training sets of approximately even size. A Random Forests with 1000 trees was trained (28). Random Forests generates three probabilities summing up to 1 for each edge: probability of being physical (RFphys), probability of being functional (RFfun) and probability of being non-related (NON). This analysis was done using the Random Forests package from R (<http://www.r-project.org/>).

The above Random Forests scores are de-novo predictions of interactions because they are not based on any data originating from experimental testing of interactions. In order to integrate prior knowledge of measured interactions we combined the Random Forests scores with experimental lines of evidence using Bayesian integration (implemented in R) as described previously (29). This approach also accounts for correlation between individual lines of evidence.

Evaluation

The different prediction strategies were computationally validated using cross-validation and using independent sets of known interactions. Five fold cross-validation was performed by randomly sampling training and test sets from the pools of reference interactions. However, cross-validation might overestimate the predictive power of machine learning methods, because it does not take into account systematic differences between independently measured data. Hence, our second strategy

hides one data source during the training phase and uses it for testing. Here, we used CRGhigh for independent testing, since it is not commonly used as a training set and so allowing it to be used as an independent test set for comparing all different networks. If a test interaction was reported in another source, it was removed from the training data and only used for testing.

Analysis of cross talk between pathways and compartments

In order to analyze the cross-talk between pathways we selected all genes annotated for at least one cellular process or environmental information processing pathway in KEGG. We generated a high confidence physical interaction network of these selected genes with interactions having a Random Forests physical interaction score above 0.7. Because many genes are annotated for more than one pathway it is non-trivial to decide if a physical interaction is within or between two pathways. Two different strategies were followed for classifying interactions as ‘between pathway’. Assume P_{g1} and P_{g2} are the sets of pathways for which the genes $g1$ and $g2$ are annotated. In the first strategy, we call the interaction $g1 - g2$ ‘between’ if $P_{g1} \cap P_{g2} = \emptyset$ and we added $\frac{1}{|P_{g1} \times P_{g2}|}$ as cross-talk for each pair of pathways in the Cartesian product $P_{g1} \times P_{g2}$. If $P_{g1} \cap P_{g2} = A \neq \emptyset$ then we treat this as a *within* interaction and we added $\frac{1}{|A|}$ contribution as *within* interaction for each pathway in A . This first approach rests on the assumption that two genes annotated for a common pathway are interacting inside that pathway. However, if genes are also annotated for different pathways the interaction may (in addition) also link those distinct pathways.

Hence, in the second strategy, even if two genes share common pathways, we assumed there is cross-talk between pathways in P_{g1} and P_{g2} . Again we add a contribution $\frac{1}{|P_{g1} \times P_{g2}|}$ as cross-talk for each pair in $P_{g1} \times P_{g2}$. Note, that in contrast to the first strategy, it is possible to have pairs (x, x) in this Cartesian product since $P_{g1} \cap P_{g2}$ is not necessarily empty. Such a pair was assumed as within interaction in pathway x . At the end, for each strategy, we generated a $N \times N$ matrix showing the cross-talk between N pathways.

We carried out the same analysis for cellular compartments. The only difference is that, instead of KEGG pathways, we used genes that have a cellular localization annotation in the generic version of *GO slim* (<http://www.geneontology.org>). Cytoscape was used for drawing the networks (30).

Selecting genes for Y2H experiments

Genes potentially related to ALS, Parkinson, Huntington or Alzheimer were selected using three data sources OMIM (<http://www.ncbi.nlm.nih.gov/omim/>, downloaded 28/10/10) KEGG (24) and GAD (31). From OMIM we selected genes that are known to be related with these diseases; for achieving maximal stringency we only selected genes from OMIM class 3: their mutations were positioned by mapping the wild type gene and a mutation in that gene created a phenotype that is in association with the disorder. GAD contains results from Genome Wide Association Studies (GWAS) and linkage studies. We selected genes from GAD that show positive association with the diseases. From KEGG we selected all genes participating in the respective disease pathways. The union of all of these genes resulted in 433 non-redundant genes (Entrez Gene IDs).

Functional Enrichment

We calculated functional enrichment (based on GO) of genes interacting with known disease associated genes (OMIM) or candidate genes (GWAS) using Fisher's exact test. The purpose was to show that 'linker genes' lying between GWAS and OMIM genes are enriched for specific molecular functions that are different from other genes neighboring OMIM genes. Hence, we did not compute the functional enrichment of linker genes versus the whole genome, but versus other neighbors of OMIM genes. Thus, enrichment of linker genes was computed using as universe not the whole genome but the whole set of OMIM or GWAS gene interactors respectively (Supplementary Tables 6, 7). However, using the whole genome as a universe yields similar findings especially in case of the OMIM interactors (Supplementary Table 8).

Central nervous system (CNS) specificity

CNS specificity for each of the interactions is calculated via applying the Kolmogorow-Smirnov (KS) test. mRNA expression levels in various human tissues were collected from BIOGPS. For each of the 12,056 genes present in the BIOGPS we compared expression in CNS tissues/cell types versus all other tissues using the KS test. Interactions were scored by assigning the lowest p-value of the two interacting genes to the edge. This is due to the fact that an interaction is present in a specific tissue only if both partners are expressed, hence it is restricted on the less promiscuous gene.

Experimental Testing of Protein Associations

Yeast two-hybrid (Y2H)

Y2H experiments were performed as described previously (7). In Brief, selected ORFs were transferred into bait (pBTM117c) and prey vectors (pACT4-DM). The L40ccU2 MATa yeast strain was transformed with the bait plasmids and preys were used to transform MAT α strain L40cc α (32). Bait and prey yeast strains were pair wise ordered in microtiter plate format according to hPRINT predictions and mated on YPD for 36h. Diploid yeast were grown on SD media supplemented with histidine and uracil for 3d. Interacting proteins were identified by growth on selective plates (-Leu-Trp-Ura-His) after 6 days. Random non interacting pairs were tested by mating non pair wise matching bait and prey plates. Every protein pair was assayed in at least two independent interaction mating experiments.

Cell line production

Mouse or human BAC harboring the genes of interest were obtained from the BACPAC Resources Center (<http://bacpac.chori.org>). The N-terminal NFLAP tagging cassette as well as the C-terminal LAP and DIGtag tagging cassettes were PCR amplified using primers that carry 50 nucleotides of homology to the N- or C-terminus, respectively, of each of the target genes. Recombineering and stable transfection of the modified BAC was performed as described (33). Briefly, both, a plasmid carrying two recombinases and the purified tagging cassette, were introduced into the E. coli strain

containing the BAC vector using electroporation. Precise incorporation of the tagging cassette was confirmed by PCR and sequencing. Next, the GFP-tagged BACs were isolated from bacteria using the Nucleobond PC100 kit (Macherey-Nagel, Germany).

Subsequently, HeLa Kyoto cells were transfected using Effectene (Qiagen) and cultivated in selection media containing 400 µg/ml geneticin (G418, Invitrogen). Finally, HeLa pools stably expressing the tagged transgenes were analyzed by western blot and immunofluorescence using an anti-GFP antibody (Roche) to verify correct protein size and localization of the tagged transgene. Next, cell pools were subject to analysis using mass spectrometry(8).

Affinity purification, mass-spectrometry protein identification (AP-MS)

Affinity purification - mass-spectrometry protein identification (AP-MS) was performed according to the recently published QUBIC (Quantitative BAC InteraCtomics) method (8). In short, pulldowns of GFP-tagged, transgenic cell line and of an untransfected control cell line were done in triplicates using monoclonal anti-GFP antibody coupled to µMACS beads (Miltenyi Biotec). Purified proteins were digested in-column and purified peptides were directly subjected to LC-MS/MS analysis using a Proxeon EASY-nLC system coupled online to a LTQ-Orbitrap. Raw data was analyzed using the MaxQuant Software (version 1.1.0.28) with label-free protein quantification (34). Significant interactors were determined by a volcano plot-based strategy, combining p-values of the standard equal group variance t-test with ratios comprised from protein intensities in the pulldowns of the transgenic and the control cell line. MaxQuant settings and significance cut-offs were chosen as described in (8).

Results

Predicting the human physical interactome

For predicting the human protein-protein interactions we developed a novel combined Random Forests / Bayesian learning strategy. First, we integrated information from automated text mining

Fig. 1

with comparative and functional genomics data, protein domain profiles and network features resulting in a total of 18 features (Fig. 1, Supplementary Table 1). This data was generated in-house (26, 27) and obtained from the STRING database (35). Because we aimed at the *de novo* prediction of binding experimental data reporting direct evidence for physical protein association was excluded at this step. Experimental binding data was however integrated at a later step for further improving the coverage and accuracy of the interaction map (see Fig. 1a and *Experimental Procedures*). We generated independent sets of positive reference interactions based on four high-confidence sources (see *Experimental Procedures*). All subsequent steps were tested independently on these positive reference sets in order to ensure generality of our findings. Random interactions between proteins that were part of the positive reference sets were used as a negative reference set. We employed the Random Forests supervised learning algorithm (28) for integrating the features and predicting interactions. An important feature of our method is the simultaneous classification of three types of protein pairs: physical binding (RFphys), functional association (RFfun) and non-related, i.e. pairs of proteins that likely do not interact. These scores reflect the probability for membership in the respective class. RFfun reflects the probability that an interaction is functional but not physical, while physical binding (high RFphys) does not preclude functional association. Note that $1 - (\text{RFfun} + \text{RFphys})$ is the probability that the respective protein pair does not interact at all. Using our pipeline we tested more than 5 million protein pairs. hPRINT predicts 94,009 new interactions ($\text{RFphys} > 0.7$) that have no prior experimental evidence in any of the databases that we included. We created a web-interface for hPRINT at www.print-db.org, allowing to search the database and to download the data.

Evaluating hPRINT

Based on the positive and negative reference interactions we subjected hPRINT to a range of tests. In addition to cross-validation, we assessed predictions based on test sets obtained from independent sources. This approach ensures that the performance assessment is independent of specificities of the training or test data. First, we compared our approach to other machine learning

Fig. 2

methods (Fig. 2a and Supplementary Fig. 1a, 2a, 3a). Random Forests clearly outperformed all other methods tested, which is consistent with previous studies (21, 36, 37). Next, we compared four published networks and hPRINT in their ability of predicting physical association of human proteins (Fig. 2b and Supplementary Fig. 1b, 2b, 3b). hPRINT performed consistently better than previous approaches. In order to show that these differences are statistically significant, we performed 5-fold cross validation, computing each time the area under the ROC curve (AUC). This provided us with distributions of AUC scores that we compared between hPRINT and STRING (which has the largest overlap with the test set among all competing databases). It turned out that the AUCs of hPRINT are significantly larger than those of STRING (t-test, $p = 6.7 \cdot 10^{-07}$) (Supplementary Table 2). In order to underline the importance of distinguishing physical from functional association we also tested if RFFun could predict known physical binding events (Fig. 2b): while RFFun is predictive for physical association, it performs much worse than RFphys.

It has recently been proposed that predicted physical interactomes can be used for streamlining the experimental mapping of interactions (13). To test this hypothesis with human proteins and to further corroborate the reliability of hPRINT we conducted experimental testing of predicted interactions using Y2H and AP-MS. For Y2H we selected 433 proteins that are known to be related to at least one of four neurodegenerative diseases (ALS, Parkinson's, Huntington and Alzheimer's, see *Experimental Procedures* for details). After removing proteins for which clones were not available in our library or which were autoactive we were left with 281 proteins, giving rise to almost 40,000 possible pairs. Of these we tested 5,434 at least twice. These interactions consist of 548 pairs with RFphys scores above 0.5, 3010 had no evidence in hPRINT, and the remaining ones have RFphys scores below 0.5. Also, this set contained 295 interactions from our positive control set, which we used for assessing the sensitivity or retest rate of the assay. Thus, our experimental test set contains various controls all based on the same 281 proteins (i.e. thereby controlling for potential protein set specific biases). We reproducibly detected 81 interactions (54 present in hPRINT), most of which were not reported before. Validation rates are substantially better for high-scoring interactions

compared to the negative controls (Figure 2c). The experimentally validated interactions have significantly higher RFphys scores compared to RFFun (Kolmogorov-Smirnov (KS) test, $p=0.0016$) and random interactions (KS test, $p=2.45\cdot 10^{-12}$). This is also true for cut-off values different than 0.5. Supplementary Figures 4 and 5 show that the predictive power increases as a function of the interaction score. Other databases also performed better than random in predicting the Y2H interactions; however, the predictive power was below that of RFphys (STRING: $p=1.25\cdot 10^{-09}$, PIP: $p=0.615$, HiMAP and FunCoup had too small overlap with the experimentally validated interactions to allow for a quantitative assessment). Hence, using hPRINT we can significantly increase the success rate for interaction screening as compared to random testing of interactions.

Next, we performed AP-MS experiments using 14 proteins with neurological relevance as baits. For these baits hPRINT predicted in total 43 interactions with a RFphys score above 0.5. In case of the AP-MS measurements the set of tested interactions was defined as the set of all predicted interactions with the respective bait protein. Between 1 and 181 proteins were co-purified per bait, resulting in a total of 462 interactions (92 present in hPRINT). Again, validation rates are much higher for RFphys than for the negative controls (Figure 2d), RFphys scores of validated interactions are significantly higher than random ($p=2.2\cdot 10^{-7}$) and higher than RFFun scores ($p=3.05\cdot 10^{-7}$, Supplementary Table 3). We also tested how well other databases could predict the experimentally verified interactions. Similar to what we observed with the Y2H test set, the comparison with other databases using the AP-MS test set shows that hPRINT performs best (Supplementary Table 3, Supplementary Fig. 4, 6). Benchmarking our predictions against another recently published set of AP-MS measurements (38) yields similar results (Supplementary Fig. 7).

Predicted Interactome Covers Many Underexplored Genes

Most existing measurements of protein-protein interactions are biased towards well-studied genes and even high-throughput screens may be biased due to the selection of bait proteins (39, 40). One goal of this study was to at least partly fill this gap by predicting interactions for less well studied genes. In order to assess the bias towards well studied genes, genes were grouped based on their

Fig. 3

citation frequency in PubMed abstracts. Figure 3 shows the number of interactions as a function of 'gene popularity'. Experimentally verified interactions (reported in HPRD, KEGG, CORUM, CRGHigh and IntAct) are biased towards well studied genes, while in hPRINT this bias is much less pronounced. hPRINT not only predicts new interactions among already well studied genes for which an abundance of information is already available. Thus, the input data used is less dependent on gene-popularity and our prediction method effectively uses this information. The importance of text mining derived features in our predictions (Fig. 1b) might suggest that our network should be subject to the same bias as experimental datasets. However, our text mining based features are normalized for the number of citations (26), which partly balances the bias against less studied genes. Additionally, our network is utilizing unbiased information such as co-expression or protein sequence, which is available for virtually all gene pairs. In conclusion our network predicts interactions for largely unexplored parts of the genome.

Networks linking cellular processes and signaling pathways

Fig. 4

Recently it has been noted that viewing signaling pathways as isolated linear chains of reactions may be misleading. Many pathways are in fact interconnected, i.e. signaling pathways are linked to other regulatory or signaling pathways and to basic cellular processes such as endocytosis (41, 42). It is emerging that cells are using highly connected networks to integrate a wide variety of noisy signals, for predicting future conditions in the environment and ultimately for balancing partly conflicting cues to make decisions (43, 44). Having a substantially more comprehensive and less biased map of the human physical interactome allows us to reexamine the degree to which proteins interact within a specific pathway and across pathways. In order to quantify the extent of inter-pathway connectivity we measured the fraction of interactions bridging different pathways (Figure 4a, Supplementary Figure 7). Likewise, we quantified the fraction of interactions connecting different cellular compartments (Figure 4b). Interactions between proteins annotated for different cellular localizations could be either due to binding at interfaces or due to multiple protein localizations. In the latter case, interactions in fact do not 'bridge' compartments, but they rather reflect the

dynamics of protein (re-)localization. Figure 4 clearly shows that the fraction of interactions connecting cellular localizations is much larger than the fraction of interactions bridging pathways. While 50% of the interactions link proteins at different localizations, 29% of the interactions connect proteins annotated for different pathways. This observation reflects the fact that most pathways span several compartments and it shows that the cellular context of proteins is very dynamic. Pathways on the other hand, representing functional sub-units of the proteome, are less densely connected between each other. Still, the fact that almost one third of all interactions are inter- rather than intra-pathway suggests considerable interconnectedness, emphasizing once more that signal processing and decision making in cells are highly inter-connected processes operating at the network level.

Using hPRINT for exploring genes associated with neurodegenerative diseases

Genome Wide Association Studies (GWAS) allow for the unbiased detection of disease modifying genes (45-47). Having identified SNPs in or close to a gene from a large population of individuals it is not always apparent what the molecular mechanisms are linking the causal gene to the disease phenotype (47). Physical protein interaction data has proven to be helpful in similar contexts, but applications to GWAS are still limited (46, 48-52). We reasoned that a network with increased coverage would also be of improved utility for studying GWAS candidate genes.

Here we address the important problem of prioritizing candidate genes identified through GWAS. Our hypothesis was that for a given disease, candidate genes whose products are closer in our network to confirmed causal disease genes are likely to have stronger effects on the disease phenotype, i.e. those genes might be more relevant and easier to replicate. For testing this hypothesis we selected the top ranking genes from AlzGene (53), a database offering a publicly available and regularly updated field-synopsis of published genetic association studies performed on Alzheimer's disease (AD). The overall epidemiological credibility of the top genes is graded as "A" (strong, 19 genes), "B" (moderate, 19 genes) and "C" (weak, 44 genes) (53). Next, we obtained a set

of high-confidence disease causing genes from Online Mendelian Inheritance in Man (OMIM) and quantified the distance between candidate genes from AlzGene and known genes from OMIM (distance was defined as the smallest sum of links connecting the respective proteins in hPRINT).

Initially, we performed the analysis using all data, i.e. combining predictive and experimental evidence (using the Bayesian scoring, Figure 1a). In our network AlzGene candidates are significantly closer to disease genes than random genes (Fig. 5A, Supplementary Table 4). Also, genes graded A generally had shorter distances to OMIM genes than genes graded B or C (though this difference was not statistically significant). Next, we tested how important the predictive evidence was for correctly ranking the candidate genes. When using experimental information alone the difference between class B and C genes and randomly selected genes vanished and only class “A” genes were still closer to OMIM genes than expected by chance (Supplementary Figure 9a, Supplementary Table 4).

Fig. 5

Another concern might be that the degree of the nodes that we assessed influenced the results (e.g. if a class A gene has a very high degree this might reduce the distance to all genes in the network). To address this problem we randomly re-wired the network maintaining the degree of each node. Such randomization diminished the differences between the gene classes (Supplementary Figure 9b) showing that the differences seen before are not an artifact caused by high node degrees. These findings suggest that network distance in hPRINT can be used for prioritizing candidate genes from GWA studies and that the predicted interactions add disease relevant information to the network. For prioritizing genes linked to three neurodegenerative diseases, we compiled 75 candidate genes for ALS, Alzheimer’s and Parkinson’s disease (54), mapped them onto hPRINT (48 out of 75) and ranked them based on their network distance to known disease genes, respectively (Supplementary Table 5). In case of AD the top scoring gene was *CLU*, which ranked second in AlzGene after *ApoE*.

The concordance between AlzGene and our network-based analysis is interesting in two respects: AlzGene is also based on an automated ranking of candidate genes. But instead of using network information it ranks genes based on their reproducibility across several genetic linkage and association studies. Hence, we achieve agreement based on complementary data. This implicates

first, that our network analysis might be particularly useful for traits with smaller numbers of independent association studies that could be used to confirm candidate genes. And second, the correlation between molecular interactions and reproducibility in association studies suggests that effect size might be a function of molecular proximity to established disease genes.

Linker Genes are enriched for Common Functions

In order to further corroborate the relevance of genes identified through the network analysis and to obtain first hints towards molecular mechanisms we analyzed the genes and interactions connecting candidate GWAS genes to known disease genes (i.e. genes from OMIM). For each candidate gene we identified its closest known disease causing gene and selected all 'linker genes' lying between these two genes in hPRINT. These linker genes are particularly interesting, because they are typically not known to affect disease phenotypes, but they may be important for understanding the disease mechanisms. These linker genes could not easily have been identified without the network information.

We assessed the relevance and consistency of linker genes by measuring the functional enrichment among them based on Gene Ontology (GO) terms. Interestingly, linker genes of all three diseases are enriched for related cellular processes (Supplementary Tables 6 & 7). Apoptosis (programmed cell death) and cytoskeleton rearrangements/cargo transportation are two terms that appear frequently among linker genes in all three diseases. These functions are clearly connected to the etiology of neurodegenerative diseases (55), further underlining the potential role of linker genes in the establishment of disease phenotypes.

Interactions Connecting Disease Genes are CNS Specific

We then calculated the central nervous system (CNS) specificity for disease genes, linker genes, and their interactions based on expression data from BIOGPS (56, 57). The CNS specificity score of interactions is based on the simple notion that both proteins constituting an interaction must be expressed in a given tissue or cell type. Hence, CNS specificity of an interaction is high when a given pair of proteins is expressed in the CNS (see *Experimental Procedures*).

We noticed that interactions between disease genes (either GWAS or OMIM) are more CNS specific than interactions involving linker genes. (Fig. 5b, c and Supplementary Fig. 10 - 13). Hence, genes with CNS specific interactions connecting to known disease genes are more likely to be of higher relevance. Supplementary Table 5 lists the top candidate disease genes interacting with known disease genes in a CNS specific manner. Based on this ranking CLU is again predicted to be one of the top candidates for Alzheimer's disease. Also Translocase of outer mitochondrial membrane 40 homolog (*TOMM40*) ranked highly as an AD candidate gene based on both the shortest path and CNS specificity scores (Supplementary Table 5). There has been a debate whether mutations in *TOMM40* are actually related with higher risk in developing Alzheimer's disease (58) or whether the correlation of *TOMM40* with Alzheimer's is due to linkage disequilibrium (59, 60). More recent work suggests that *TOMM40* is indeed involved in AD etiology (61) and our findings support this view.

We also noticed that interactions derived by applying the shortest path algorithm, though they are not all CNS specific, cluster various tissues and especially CNS successfully (Fig. 5c). This observation implies that the physiological differences between tissues are not due to a large fraction of tissue specific proteins (62). Rather, tissue specificity seems to be achieved through activation of a specific set of interactions or protein complexes (Fig. 5c and Supplementary Fig. 12, 13).

Discussion

hPRINT uses a combination of Random Forests and Bayesian learning approaches in order to integrate various types of evidence for predicting physical protein interactions and integrating those predictions with known information. This unique combination of machine learning methods, the emphasis on distinguishing physical binding from functional association, the coverage of the human genome, and the extensive experimental testing of our predictions set hPRINT apart from existing resources.

The specific design of our prediction pipeline combines the following goals: (i) it makes robust predictions even in the complete absence of experimental binding evidence; (ii) because using Random Forests it allows for non-linear interactions between the features; (iii) final interaction scores also include published experimental evidence. Other designs would have failed to meet at least one of these criteria. For example, including experimental evidence in the first step (and thus dropping the second Bayesian learning step) would potentially have led to circular reasoning. An additional more subtle disadvantage is that in that case Random Forests would have given strong preference to experimental evidence since it almost perfectly predicts binding in the training set. Thus, other types of evidence that are needed for actual predictions would not have been trained correctly for situations when experimental evidence is absent. Our two-step procedure circumvents both of these problems.

When assembling the reference interactions that we used for training and testing we have tried to avoid circular reasoning as much as possible especially by excluding experimental evidence. However, complete independence from all the information we used for predicting interactions is not possible (e.g. in the case of text mining). Essentially all published predicted networks suffer from this limitation. We addressed this problem in two different ways: first, we removed all text mining-based features and second, we conducted independent experimental testing. Supplementary Figure 15 shows that the quality of the predictions does not drop when removing text mining-based features, even though, of course, the density of the network is reduced. This analysis confirms that the quality

measures shown in Figure 2 are not biased in favor of the predictions due to potential circular reasoning when using text mining. Independent experimental testing should address all possible biases – even undetected ones. We evaluated hPRINT and the other databases based on three new experimental datasets: one was very recently published and not available for the training of hPRINT (38), and two novel screens were performed in the framework of this project and are reported here. Using the two complementary experimental methods, Y2H and AP-MS, we demonstrated the predictive power of hPRINT and we confirmed the importance of distinguishing physical and functional gene associations. In addition, in our experiments we tested the performance of hPRINT and other databases using large scale screening setups. We set out to experimentally test hPRINT predictions with standardized experimental setups rather than testing our method using literature-derived gold standards.

Initially, it might be surprising that the Y2H experiments identified only 81 interactions among 5,434 tested protein pairs. However in such an approach it is very important to test a large number of non interacting pairs as well as the predicted interactions, because we anticipated an extremely low success rate in the negative/random control set (5). Therefore, by design only half of the tested interactions had any prediction score in our database and only 548 had an RFphys score above 0.5. Since *in vivo* interactions often depend on specific cellular conditions (e.g. presence of co-factors) we do not expect that all predicted interactions can be verified using these standardized high throughput assays. In fact, our validation rate compares well to the retest rate for the positive reference set (Figure 2c+d), indicating that the low sensitivity of the experimental techniques accounts for the relatively low number of interactions found rather than the false positive rate of the hPRINT predictions. Hence, these experiments do not serve to provide validation of individual interactions, but they provide very good support for a quality assessment of the hPRINT predictions and other databases in a quantitative and unbiased way. The main finding from these experiments is that the recovery rate of predictions from other databases (Supplementary Table 3) or using RFfun (Figure 2 c + d) is significantly lower than from RFphys predications. Even though some of the

experimentally observed binding events might not constitute true *in vivo* interactions and some of the interactions found in the negative sets might be actually true interactions the overall statistics would not change significantly – especially the relative differences between the networks would not change. This notion is supported by the statistical significance of the performance differences, which also reflects robustness against noise in the measurements.

The superior performance of hPRINT compared to previous attempts in predicting protein-protein binding is explained by four facts. First, the Random Forests machine learning method is more flexible than competing methods and it makes significantly fewer assumptions about the nature of the predictors and their relationships to each other. Second, the complete exclusion of experimental binding evidence in the training phase is important for robust *de novo* prediction of protein binding. Third, we are using additional features such as the network features that have not been used in combination before. Fourth, the distinction of functional and physical interactions in the machine learning turned out to be very important. Though being intuitive, this distinction has not always been made in the past. That is not to say that predicting functional relationships is useless (52). Rather, they reflect different aspects of the system and explicitly distinguishing those aids subsequent analyses built on top of the network.

Our analysis of disease association data shows that dense networks like hPRINT might improve candidate gene prioritization and assist in inferring molecular mechanisms. For example the fact that several linker genes are known to be disease related even though that information was not used in our analysis demonstrates the utility of network-based methods for identifying relevant genes. In that respect, this study represents a proof of principle.

By integrating known with high-confidence predicted interactions we almost double the currently known physical interactome. We anticipate that this resource will be instrumental for directing future screening of interactions and for conducting systems-level analysis of cellular

processes. In particular, hPRINT will be valuable for studying disease mechanisms and for short listing candidate genes identified on a genetic basis such as GWAS.

Acknowledgements

We thank Anne Tuukkanen (Technische Universität Dresden, Germany) for help with the analysis of domain motives. We acknowledge funding from the following sources: Klaus Tschira Foundation, European Community's Seventh Framework Programme (PhenOxiGen FP7-223539, Ponte FP7-247945, SyBoSS FP7-242129), German BMBF (NGFNp NeuroNet-TP3 01GS08171 (to U.S.), DiGtoP 01GS0859), German BMWi (GeneCloud), and the Max Planck Society.

References

1. Beyer, A., Bandyopadhyay, S., and Ideker, T. (2007) Integrating physical and genetic maps: from genomes to interaction networks. *Nat Rev Genet* 8, 699-710.
2. Stumpf, M., Thorne, T., Silva, E., Stewart, R., An, H., Lappe, M., and Wiuf, C. (2008) Estimating the size of the human interactome. *Proc Natl Acad Sci U S A* 105, 6959-6964.
3. Gunsalus, K. C., Ge, H., Schetter, A. J., Goldberg, D. S., Han, J.-D. J., Hao, T., Berriz, G. F., Bertin, N., Huang, J., Chuang, L.-S., Li, N., Mani, R., Hyman, A. A., Sönnichsen, B., Echeverri, C. J., Roth, F. P., Vidal, M., and Piano, F. (2005) Predictive models of molecular machines involved in *Caenorhabditis elegans* early embryogenesis. *Nature* 436, 861-865.
4. Bork, P., Jensen, L. J., von Mering, C., Ramani, A. K., Lee, I., and Marcotte, E. M. (2004) Protein interaction networks from yeast to human. *Curr Opin Struct Biol* 14, 292-299.
5. Venkatesan, K., Rual, J.-F., Vazquez, A., Stelzl, U., Lemmens, I., Hirozane-Kishikawa, T., Hao, T., Zenkner, M., Xin, X., Goh, K.-I., Yildirim, M., Simonis, N., Heinzmann, K., Gebreab, F., Sahalie, J., Cevik, S., Simon, C., Smet, A.-S., Dann, E., Smolyar, A., Vinayagam, A., Yu, H., Szeto, D., Borick, H., Dricot, A., Klitgord, N., Murray, R., Lin, C., Lalowski, M., Timm, J., Rau, K., Boone, C., Braun, P., Cusick, M., Roth, F., Hill, D., Tavernier, J., Wanker, E., Barabási, A.-L., and Vidal, M. (2009) An empirical framework for binary interactome mapping. *Nat Methods* 6, 83-90.
6. Rual, J. F., Venkatesan, K., Hao, T., Hirozane-Kishikawa, T., Dricot, A., Li, N., Berriz, G. F., Gibbons, F. D., Dreze, M., Ayivi-Guedehoussou, N., Klitgord, N., Simon, C., Boxem, M., Milstein, S., Rosenberg, J., Goldberg, D. S., Zhang, L. V., Wong, S. L., Franklin, G., Li, S., Albala, J. S., Lim, J., Fraughton, C., Llamas, E., Cevik, S., Bex, C., Lamesch, P., Sikorski, R. S., Vandenhaute, J., Zoghbi, H. Y., Smolyar, A., Bosak, S., Sequerra, R., Doucette-Stamm, L., Cusick, M. E., Hill, D. E., Roth, F. P., and Vidal, M. (2005) Towards a proteome-scale map of the human protein-protein interaction network. *Nature* 437, 1173-1178.
7. Stelzl, U., Worm, U., Lalowski, M., Haenig, C., Brembeck, F. H., Goehler, H., Stroedicke, M., Zenkner, M., Schoenherr, A., Koeppen, S., Timm, J., Mintzlauff, S., Abraham, C., Bock, N., Kietzmann, S., Goedde, A., Toksöz, E., Droege, A., Krobitsch, S., Korn, B., Birchmeier, W., Lehrach, H., and Wanker, E. E. (2005) A human protein-protein interaction network: a resource for annotating the proteome. *Cell* 122, 957-968.
8. Hubner, N., Bird, A., Cox, J., Splettstoesser, B., Bandilla, P., Poser, I., Hyman, A., and Mann, M. (2010) Quantitative proteomics combined with BAC TransgeneOmics reveals in vivo protein interactions. *J Cell Biol* 189, 739-754.
9. Ewing, R. M., Chu, P., Elisma, F., Li, H., Taylor, P., Climie, S., McBroom-Cerajewski, L., Robinson, M. D., O'Connor, L., Li, M., Taylor, R., Dharsee, M., Ho, Y., Heilbut, A., Moore, L., Zhang, S., Ornatsky, O., Bukhman, Y. V., Ethier, M., Sheng, Y., Vasilescu, J., Abu-Farha, M., Lambert, J. P., Duewel, H. S., Stewart, Kuehl, B., Hogue, K., Colwill, K., Gladwish, K., Muskat, B., Kinach, R., Adams, S. L., Moran, M. F., Morin, G. B., Topaloglou, T., and Figeys, D. (2007) Large-scale mapping of human protein-protein interactions by mass spectrometry. *Mol Syst Biol* 3, 89.
10. Ramirez, F., Schlicker, A., Assenov, Y., Lengauer, T., and Albrecht, M. (2007) Computational analysis of human protein interaction networks. *Proteomics* 7, 2541-2552.
11. Stelzl, U., and Wanker, E. (2006) The value of high quality protein-protein interaction networks for systems biology. *Curr Opin Chem Biol* 10, 551-558.
12. Pitre, S., Alamgir, M., Green, J., Dumontier, M., Dehne, F., and Golshani, A. (2008) Computational methods for predicting protein-protein interactions. *Adv Biochem Eng Biotechnol* 110, 247-267.
13. Schwartz, A., Yu, J., Gardenour, K., Finley, R., and Ideker, T. (2009) Cost-effective strategies for completing the interactome. *Nat Methods* 6, 55-61.
14. McDermott, J., Guerquin, M., Frazier, Z., Chang, A. N., and Samudrala, R. (2005) BIONEER: enhancements to the framework for structural, functional and contextual modeling of proteins and proteomes. *Nucleic Acids Res* 33, W324-325.

15. Rhodes, D. R., Tomlins, S. A., Varambally, S., Mahavisno, V., Barrette, T., Kalyana-Sundaram, S., Ghosh, D., Pandey, A., and Chinnaiyan, A. M. (2005) Probabilistic model of the human protein-protein interaction network. *Nat Biotechnol* 23, 951-959.
16. Jensen, L., Kuhn, M., Stark, M., Chaffron, S., Creevey, C., Muller, J., Doerks, T., Julien, P., Roth, A., Simonovic, M., Bork, P., and Mering, C. (2009) STRING 8: a global view on proteins and their functional interactions in 630 organisms. *Nucleic Acids Res* 37, D412-416.
17. Brown, K. R., and Jurisica, I. (2005) Online predicted human interaction database. *Bioinformatics* 21, 2076-2082.
18. Lefebvre, C., Rajbhandari, P., Alvarez, M. J., Bandaru, P., Lim, W. K., Sato, M., Wang, K., Sumazin, P., Kustagi, M., Bisikirska, B. C., Basso, K., Beltrao, P., Krogan, N., Gautier, J., Dalla-Favera, R., and Califano, A. (2010) A human B-cell interactome identifies MYB and FOXM1 as master regulators of proliferation in germinal centers. *Mol Syst Biol* 6, 377.
19. McDowall, M., Scott, M., and Barton, G. (2009) PIPs: human protein-protein interaction prediction database. *Nucleic Acids Res* 37, D651-656.
20. Alexeyenko, A., and Sonnhammer, E. L. (2009) Global networks of functional coupling in eukaryotes from comprehensive data integration. *Genome Res* 19, 1107-1116.
21. Qi, Y., Bar-Joseph, Z., and Klein-Seetharaman, J. (2006) Evaluation of different biological data and computational classification methods for use in protein interaction prediction. *Proteins* 63, 490-500.
22. Keshava Prasad, T. S., Goel, R., Kandasamy, K., Keerthikumar, S., Kumar, S., Mathivanan, S., Telikicherla, D., Raju, R., Shafreen, B., Venugopal, A., Balakrishnan, L., Marimuthu, A., Banerjee, S., Somanathan, D., Sebastian, A., Rani, S., Ray, S., Harrys Kishore, C. J., Kanth, S., Ahmed, M., Kashyap, M., Mohmood, R., Ramachandra, Y. L., Krishna, V., Rahiman, A., Mohan, S., Ranganathan, P., Ramabadran, S., Chaerkady, R., and Pandey, A. (2009) Human Protein Reference Database--2009 update. *Nucleic Acids Res* 37, D767-772.
23. Ruepp, A., Brauner, B., Dunger-Kaltenbach, I., Frishman, G., Montrone, C., Stransky, M., Waegle, B., Schmidt, T., Doudieu, O., Stümpflen, V., and Mewes, W. (2008) CORUM: the comprehensive resource of mammalian protein complexes. *Nucleic Acids Res* 36, D646-650.
24. Kanehisa, M., Goto, S., Furumichi, M., Tanabe, M., and Hirakawa, M. (2010) KEGG for representation and analysis of molecular networks involving diseases and drugs. *Nucleic Acids Res* 38, D355-360.
25. Bossi, A., and Lehner, B. (2009) Tissue specificity and the human protein interaction network. *Mol Syst Biol* 5, 260.
26. Plake, C., Royer, L., Winnenburger, R., Hakenberg, J., and Schroeder, M. (2009) GoGene: gene annotation in the fast lane. *Nucleic Acids Res* 37, W300-304.
27. Henschel, A., Winter, C., Kim, W. K., and Schroeder, M. (2007) Using structural motif descriptors for sequence-based binding site prediction. *BMC Bioinformatics* 8 Suppl 4, S5.
28. Breiman, L. (2004) Random Forests. *Machine Learning* 45, 5-32.
29. Elefsinioti, A., Ackermann, M., and Beyer, A. (2009) Accounting for redundancy when integrating gene interaction databases. *PLoS One* 4, e7492.
30. Cline, M., Smoot, M., Cerami, E., Kuchinsky, A., Landys, N., Workman, C., Christmas, R., Avila-Campilo, I., Creech, M., Gross, B., Hanspers, K., Isserlin, R., Kelley, R., Killcoyne, S., Lotia, S., Maere, S., Morris, J., Ono, K., Pavlovic, V., Pico, A., Vailaya, A., Wang, P.-L., Adler, A., Conklin, B., Hood, L., Kuiper, M., Sander, C., Schmulevich, I., Schwikowski, B., Warner, G., Ideker, T., and Bader, G. (2007) Integration of biological networks and gene expression data using Cytoscape. *Nat Protoc* 2, 2366-2382.
31. Becker, K. G., Barnes, K. C., Bright, T. J., and Wang, S. A. (2004) The genetic association database. *Nat Genet* 36, 431-432.
32. Goehler, H., Lalowski, M., Stelzl, U., Waelter, S., Stroedicke, M., Worm, U., Droege, A., Lindenberg, K., Knoblich, M., Haenig, C., Herbst, M., Suopanki, J., Scherzinger, E., Abraham, C., Bauer, B., Hasenbank, R., Fritzsche, A., Ludewig, A., Büssow, K., Buessow, K., Coleman, S., Gutekunst, C.-A., Landwehrmeyer, B., Lehrach, H., and Wanker, E. (2004) A protein interaction network links GIT1, an enhancer of huntingtin aggregation, to Huntington's disease. *Mol Cell* 15, 853-865.

33. Poser, I., Sarov, M., Hutchins, J., Hériché, J.-K., Toyoda, Y., Pozniakovsky, A., Weigl, D., Nitzsche, A., Hegemann, B., Bird, A., Pelletier, L., Kittler, R., Hua, S., Naumann, R., Augsburg, M., Sykora, M., Hofemeister, H., Zhang, Y., Nasmyth, K., White, K., Dietzel, S., Mechtler, K., Durbin, R., Stewart, F., Peters, J.-M., Buchholz, F., and Hyman, A. (2008) BAC TransgeneOmics: a high-throughput method for exploration of protein function in mammals. *Nat Methods* 5, 409-415.
34. Cox, J., and Mann, M. (2008) MaxQuant enables high peptide identification rates, individualized p.p.b.-range mass accuracies and proteome-wide protein quantification. *Nat Biotechnol* 26, 1367-1372.
35. Snel, B., Lehmann, G., Bork, P., and Huynen, M. A. (2000) STRING: a web-server to retrieve and display the repeatedly occurring neighbourhood of a gene. *Nucleic Acids Res* 28, 3442-3444.
36. Lin, N., Wu, B., Jansen, R., Gerstein, M., and Zhao, H. (2004) Information assessment on predicting protein-protein interactions. *BMC Bioinformatics* 5, 154.
37. Qi, Y., Dhiman, H. K., Bhola, N., Budyak, I., Kar, S., Man, D., Dutta, A., Tirupula, K., Carr, B. I., Grandis, J., Bar-Joseph, Z., and Klein-Seetharaman, J. (2009) Systematic prediction of human membrane receptor interactions. *Proteomics* 9, 5243-5255.
38. Hutchins, J., Toyoda, Y., Hegemann, B., Poser, I., Heriche, J.-K., Sykora, M., Augsburg, M., Hudecz, O., Buschhorn, B., Bulkescher, J., Conrad, C., Comartin, D., Schleiffer, A., Sarov, M., Pozniakovsky, A., Slabicki, M., Schloissnig, S., Steinmacher, I., Leuschner, M., Ssykor, A., Lawo, S., Pelletier, L., Stark, H., Nasmyth, K., Ellenberg, J., Durbin, R., Buchholz, F., Mechtler, K., Hyman, A., and Peters, J.-M. (2010) Systematic Analysis of Human Protein Complexes Identifies Chromosome Segregation Proteins. *Science* 328, 593-599.
39. Iossifov, I., Rodriguez-Esteban, R., Mayzus, I., Millen, K., and Rzhetsky, A. (2009) Looking at cerebellar malformations through text-mined interactomes of mice and humans. *PLoS Comput Biol* 5.
40. Cokol, M., Iossifov, I., Weinreb, C., and Rzhetsky, A. (2005) Emergent behavior of growing knowledge about molecular interactions. *Nat Biotechnol* 23, 1243-1247.
41. Sorkin, A., and von Zastrow, M. (2009) Endocytosis and signalling: intertwining molecular networks. *Nat Rev Mol Cell Biol* 10, 609-622.
42. Kestler, H., and Kühl, M. (2008) From individual Wnt pathways towards a Wnt signalling network. *Philos Trans R Soc Lond B Biol Sci* 363, 1333-1347.
43. Perkins, T., and Swain, P. (2009) Strategies for cellular decision-making. *Mol Syst Biol* 5, 326.
44. Hyduke, D., and Palsson, B. (2010) Towards genome-scale signalling-network reconstructions. *Nat Rev Genet* 11, 297-307.
45. Frazer, K., Murray, S., Schork, N., and Topol, E. (2009) Human genetic variation and its contribution to complex traits. *Nat Rev Genet* 10, 241-251.
46. Wu, X., Jiang, R., Zhang, M., and Li, S. (2008) Network-based global inference of human disease genes. *Mol Syst Biol* 4, 189.
47. Cordell, H. (2009) Detecting gene-gene interactions that underlie human diseases. *Nat Rev Genet* 10, 392-404.
48. Lage, K., Karlberg, O., Størling, Z., Olason, P., Pedersen, A., Rigina, O., Hinsby, A., Tümer, Z., Pociot, F., Tommerup, N., Moreau, Y., and Brunak, S. (2007) A human phenome-interactome network of protein complexes implicated in genetic disorders. *Nat Biotechnol* 25, 309-316.
49. Bergholdt, R., Størling, Z. M., Lage, K., Karlberg, E. O., Olason, P. I., Aalund, M., Nerup, J., Brunak, S., Workman, C. T., and Pociot, F. (2007) Integrative analysis for finding genes and networks involved in diabetes and other complex diseases. *Genome Biol* 8, R253.
50. Linghu, B., Snitkin, E., Hu, Z., Xia, Y., and Delisi, C. (2009) Genome-wide prioritization of disease genes and identification of disease-disease associations from an integrated human functional linkage network. *Genome Biol* 10, R91.
51. Thomas, D. (2010) Methods for investigating gene-environment interactions in candidate pathway and genome-wide association studies. *Annu Rev Public Health* 31, 21-36.
52. Lee, I., Lehner, B., Vavouri, T., Shin, J., Fraser, A. G., and Marcotte, E. M. (2010) Predicting genetic modifier loci using functional gene networks. *Genome Res* 20, 1143-1153.

53. Bertram, L., McQueen, M., Mullin, K., Blacker, D., and Tanzi, R. (2007) Systematic meta-analyses of Alzheimer disease genetic association studies: the AlzGene database. *Nat Genet* 39, 17-23.
54. Hindorff, L., Sethupathy, P., Junkins, H., Ramos, E., Mehta, J., Collins, F., and Manolio, T. (2009) Potential etiologic and functional implications of genome-wide association loci for human diseases and traits. *Proc Natl Acad Sci U S A* 106, 9362-9367.
55. Grünblatt, E. (2008) Commonalities in the genetics of Alzheimer's disease and Parkinson's disease. *Expert Rev Neurother* 8, 1865-1877.
56. Wu, C., Orozco, C., Boyer, J., Leglise, M., Goodale, J., Batalov, S., Hodge, C., Haase, J., Janes, J., Huss, J., and Su, A. (2009) BioGPS: an extensible and customizable portal for querying and organizing gene annotation resources. *Genome Biol* 10, R130.
57. Su, A., Wiltshire, T., Batalov, S., Lapp, H., Ching, K., Block, D., Zhang, J., Soden, R., Hayakawa, M., Kreiman, G., Cooke, M., Walker, J., and Hogenesch, J. (2004) A gene atlas of the mouse and human protein-encoding transcriptomes. *Proc Natl Acad Sci U S A* 101, 6062-6067.
58. Devi, L., Prabhu, B., Galati, D., Avadhani, N., and Anandatheerthavarada, H. (2006) Accumulation of amyloid precursor protein in the mitochondrial import channels of human Alzheimer's disease brain is associated with mitochondrial dysfunction. *J Neurosci* 26, 9057-9068.
59. Yu, C.-E., Seltman, H., Peskind, E., Galloway, N., Zhou, P., Rosenthal, E., Wijsman, E., Tsuang, D., Devlin, B., and Schellenberg, G. (2007) Comprehensive analysis of APOE and selected proximate markers for late-onset Alzheimer's disease: patterns of linkage disequilibrium and disease/marker association. *Genomics* 89, 655-665.
60. Bu, G. (2009) Apolipoprotein E and its receptors in Alzheimer's disease: pathways, pathogenesis and therapy. *Nat Rev Neurosci* 10, 333-344.
61. Roses, A. D., Lutz, M. W., Amrine-Madsen, H., Saunders, A. M., Crenshaw, D. G., Sundseth, S. S., Huentelman, M. J., Welsh-Bohmer, K. A., and Reiman, E. M. (2010) A TOMM40 variable-length polymorphism predicts the age of late-onset Alzheimer's disease. *Pharmacogenomics J* 10, 375-384.
62. Pontén, F., Gry, M., Fagerberg, L., Lundberg, E., Asplund, A., Berglund, L., Oksvold, P., Björling, E., Hober, S., Kampf, C., Navani, S., Nilsson, P., Ottosson, J., Persson, A., Wernérus, H., Wester, K., and Uhlén, M. (2009) A global view of protein expression in human cells, tissues, and organs. *Mol Syst Biol* 5, 337.

Figure Captions

Figure 1

(a) Workflow and **(b)** feature importance for predicting interactions.

In a first step Random Forests physical and functional interactions scores are estimated excluding direct experimental evidence. Features based on experimental evidence are weighted using a Bayesian approach and respective log-likelihood scores are computed. In a second step Random Forests physical (RFphys) and log-likelihood scores from experimental interactions are combined through Bayesian learning in order to give a final score for each interaction. **(b)** Feature importance for Random Forests machine learning expressed as the mean decrease of accuracy when shuffling the respective line of evidence. Some features are predictive but have low feature importance because of low coverage (e.g. *Gene Fusion*).

Figure 2

Evaluation of hPRINT. (a) Precision-Recall curves for comparing Random Forest with naïve Bayesian prediction and Support Vector Machines (SVM). Radial basis factor was used as kernel for training the SVM. (b) Precision-Recall curves for comparing Random Forests physical and functional scores with other published networks. The aim of the Random Forests machine learning was the *de novo* prediction of new interactions; hence, experimental interaction measurements were ignored. In the comparison we also removed experimental evidence from the other data sets. This was also necessary to avoid circular reasoning. Panels (a) and (b) are both based on 5-fold cross validation using functional and non-interacting gene pairs (FUNSET and NONSET) together as the negative dataset. Supplementary Figure 1 shows equivalent plots when using other combinations of training and test sets. (c-e) Area Under the ROC Curve (AUC) for (c) 5-fold cross validation, (b) using HPRD as an independent test set, (e) using CRGhigh as an independent test set. The AUC of RFphys is significantly larger than in all the other cases (Supplementary Figure 2, Supplementary Table 3). (f+g) Experimental validation using yeast two-hybrid (f) and AP-MS (g). High scoring interactions (RFphys > 0.5) could be confirmed with much higher probability than interactions without any evidence ('Not in hPRINT'), low scoring interactions (RFphys ≤ 0.5) and interactions predicted to be only functional (RFfun > 0.5). The comparison with the reference set ('Gold Standard') is a measure of the sensitivity of the assays. Note that in case of AP-MS we cannot define a 'Not in hPRINT' set. See **Supplementary Material** for additional analyses of the experimental testing.

Figure 3

Publication Bias. The gene name citation frequency in PubMed abstracts is shown along both axes and genes were grouped in even-sized bins. The color in each grid cell encodes the number of interactions connecting the respective gene products in the two corresponding bins. The upper triangle shows the number of experimentally tested interactions per bin pair; the lower triangle shows the number of predicted interactions in hPRINT (mean RF score per bin). The predicted interactome covers the human genome much more evenly than the known (experimentally tested) interactions, which are heavily biased towards well studied genes (bottom left corner).

Figure 4

Fraction of physical interactions connecting (a) pathways and (b) cellular locations. Each pair of pathways or cellular locations is connected by an edge reflecting the fraction of interactions from the smaller of the two groups linking proteins in those groups ('between interactions'). The size of each node shows the number of proteins annotated for that group and the nodes' border thickness is proportional to the fraction of interactions connecting proteins inside each group ('within interactions'). Note that the two panels are at scale, i.e. pathways generally have fewer annotated proteins than cellular locations. Edges with scores below 0.14 are not shown for the sake of simplicity. The full networks have many more edges, e.g. there are physical interactions connecting the Wnt-pathway with cell adhesion.

Figure 5**Prioritization of Alzheimer's disease candidate genes.**

(a) Empirical cumulative distribution function (ECDF) for the weighted network distance between OMIM genes that are known to cause Alzheimer's and candidate genes with different confidence scores (classes A – C). The distance between class A genes and OMIM genes is generally closer than in case of the other two classes or random genes. The Wilcoxon rank test was used for comparing network distances against distances for random genes. **(b)** Expression specificity in the central nervous system (CNS) quantified as the maximum specificity (minimum p-value) of the two interacting genes (see *Experimental Procedures* for details). Box-plots of CNS specificity are shown for interactions connecting different types of genes (see labels at bottom). CNS specificity is generally higher (low p-values) for interactions connecting two disease genes compared to interactions connecting disease genes with other genes. **(c)** Expression specificity of individual interactions across tissues. Each column in the heat map shows the expression of one interaction across all tissues tested. CNS specificity is shown in the top bar. Interactions were grouped in different classes based on the disease classification of the genes (vertical bands, see color code on top). Tissues (rows) were grouped according to the BIOGPS classification (color code on the left). Dendrogram on the left shows clustering of tissues based on expression specificity of the interactions. Resulting groups agree with the BIOGPS classification. Equivalent figures for ALS and Parkinson's are shown in the supplement (Supplementary Figures 9 – 12).

Figure 1

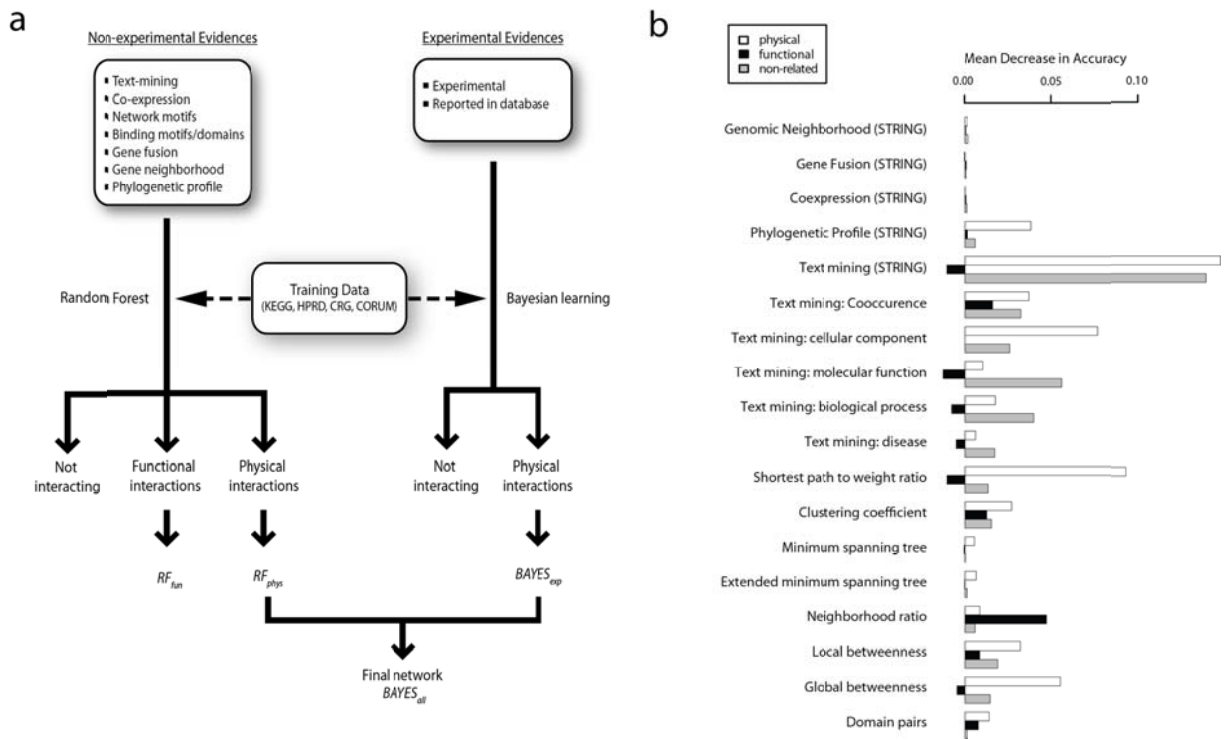


Figure 2

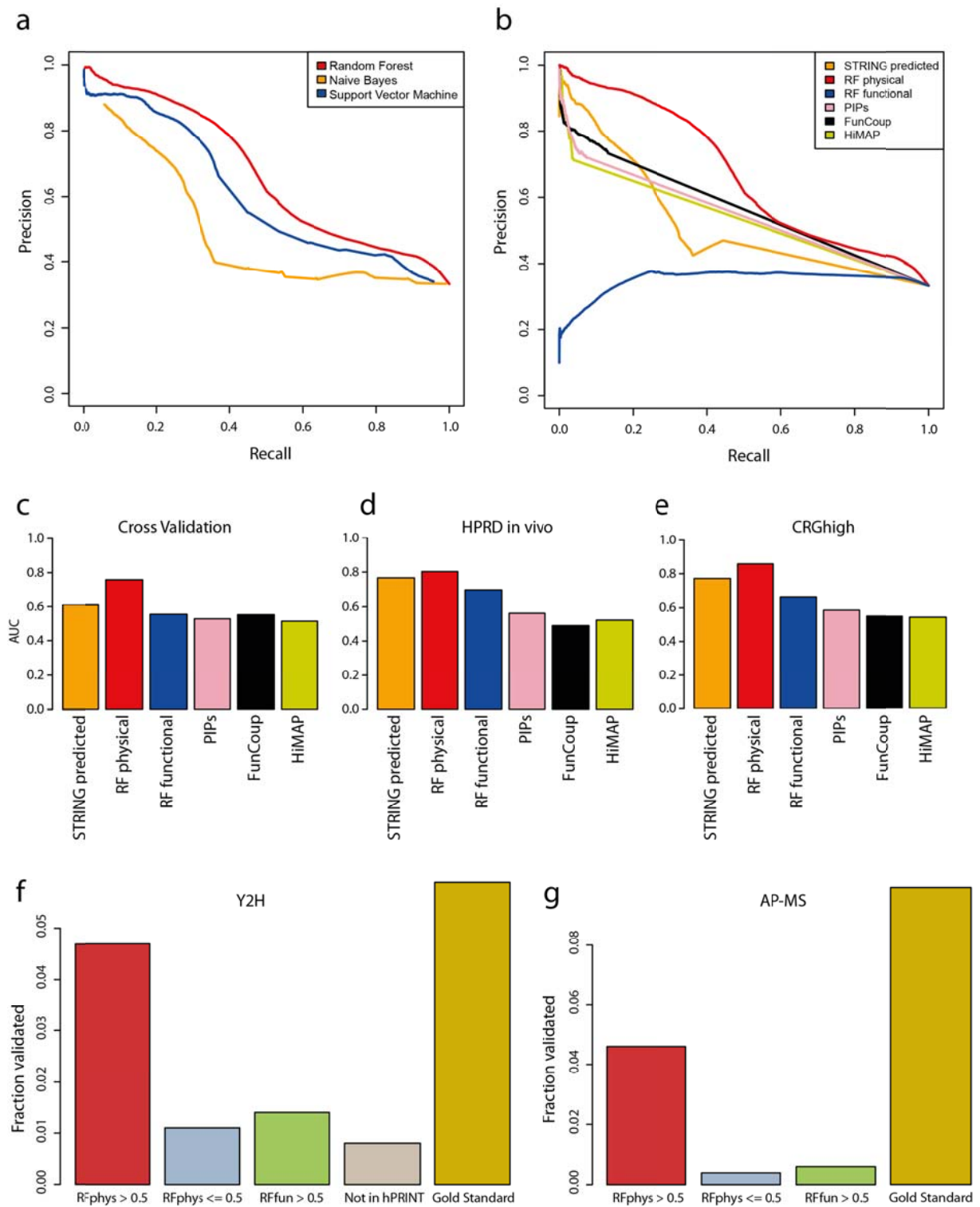


Figure 3

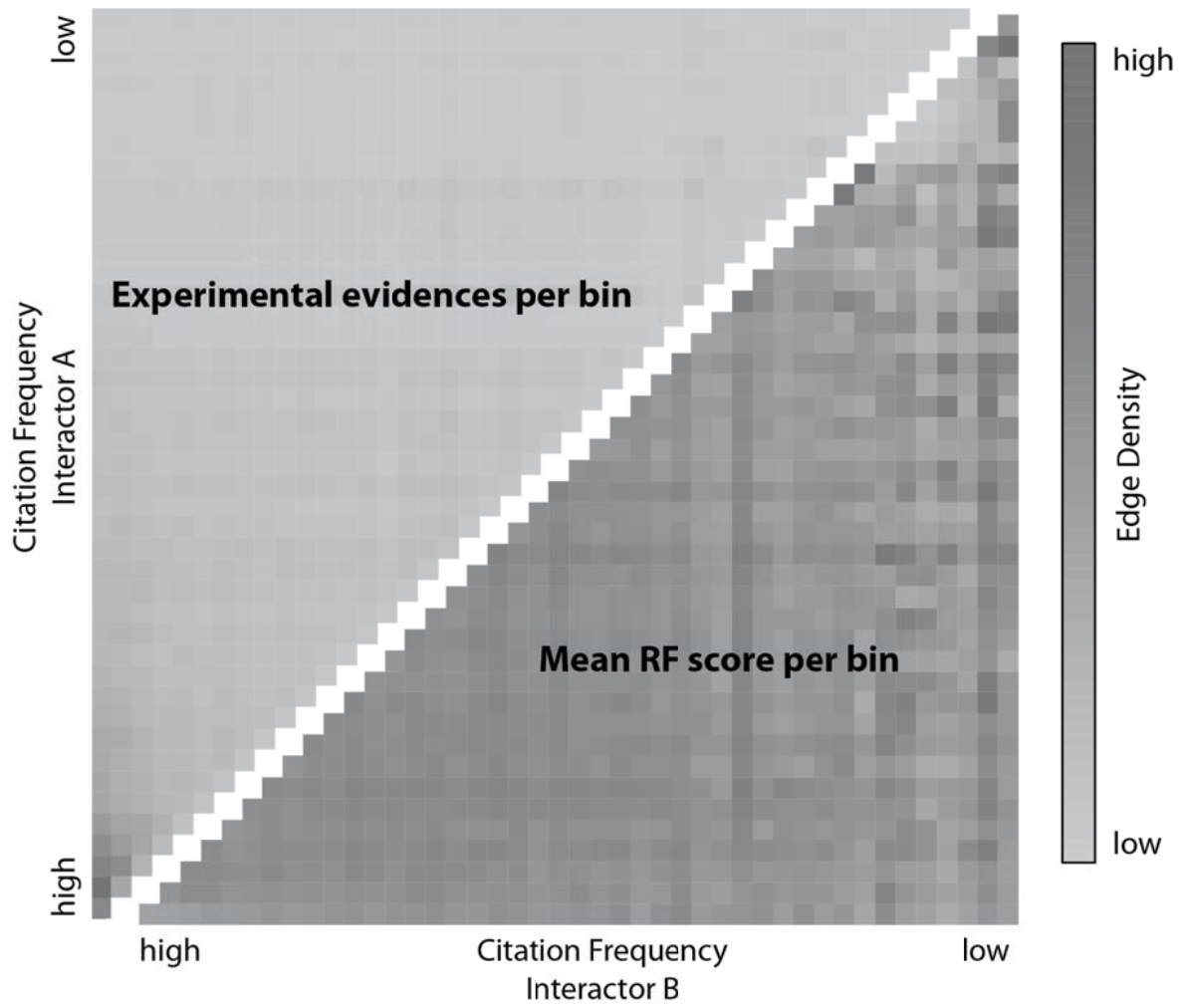


Figure 4

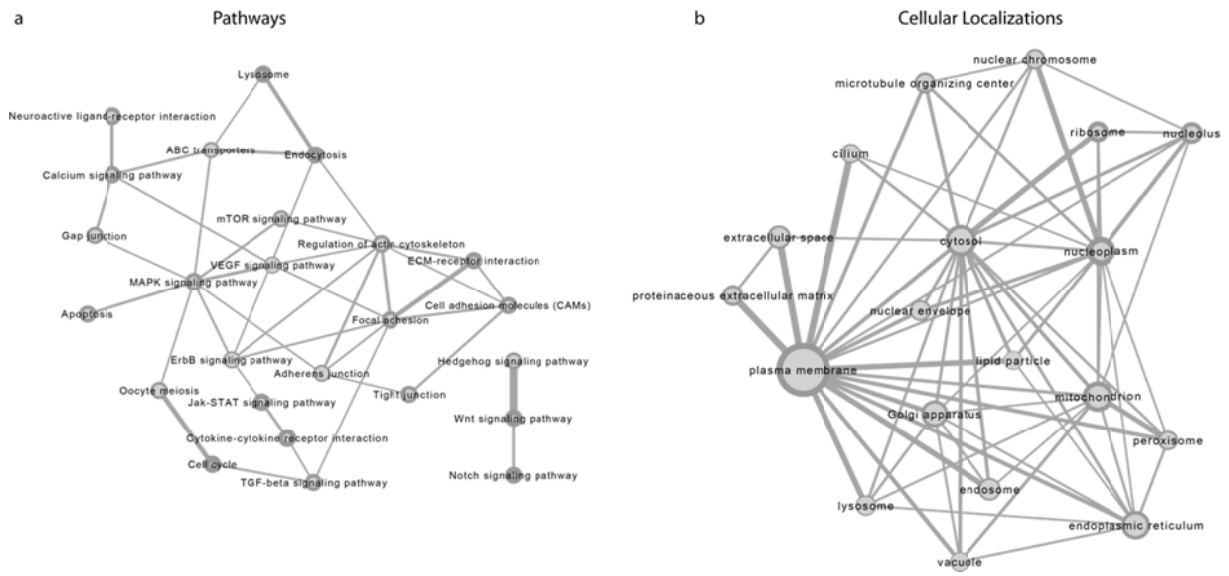


Figure 5

